Published in final edited form as:
Clin Cancer Res. 2014 June 1; 20(11): 2898–2909. doi:10.1158/1078-0432.CCR-13-3052.

Targetable signaling pathway mutations are associated with malignant phenotype in *IDH*-mutant gliomas

Hiroaki Wakimoto[1,7,8], **Shota Tanaka**[2,7,8], **William T. Curry**[1,8], **Franziska Loebel**[1,7,8], **Dan Zhao**[2,7,8], **Kensuke Tateishi**[1,7,8], **Juxiang Chen**[3,7,8], **Lindsay K. Klofas**[2,7,8], **Nina Lelic**[1,7,8], **James C. Kim**[4,8], **Dora Dias-Santagata**[3,8], **Leif W. Ellisen**[3,8], **Darrell R. Borger**[3,8], **Sarah-Maria Fendt**[6], **Matthew G. Vander Heiden**[5], **Tracy T. Batchelor**[2,7,8], **A. John Iafrate**[3,4,8], **Daniel P. Cahill**[1,7,8,*], and **Andrew S. Chi**[2,7,8,*]

[1] Department of Neurosurgery, Massachusetts Institute of Technology, Cambridge, MA, USA

[2] Stephen E. and Catherine Pappas Center for Neuro-Oncology, Division of Hematology/Oncology, Department of Neurology, Massachusetts Institute of Technology, Cambridge, MA, USA

[3] Translational Research Laboratory, Massachusetts Institute of Technology, Cambridge, MA, USA

[4] Department of Pathology, Massachusetts Institute of Technology, Cambridge, MA, USA

[5] Koch Institute for Integrative Cancer Research, Massachusetts Institute of Technology, Cambridge, MA, USA

[6] Vesalius Research Center, VIB, and Department of Oncology, KU Leuven, Leuven, Belgium

[7] Translational Neuro-Oncology Laboratory, Harvard Medical School, Boston, MA, USA

[8] Massachusetts General Hospital Cancer Center, Harvard Medical School, Boston, MA, USA

Abstract

PURPOSE—Isocitrate dehydrogenase (*IDH*) gene mutations occur in low-grade and high-grade gliomas. We sought to identify the genetic basis of malignant phenotype heterogeneity in *IDH*-mutant gliomas.

METHODS—We prospectively implanted tumor specimens from 20 consecutive *IDH1*-mutant glioma resections into mouse brains and genotyped all resection specimens using a CLIA-certified molecular panel. Gliomas with cancer driver mutations were tested for sensitivity to targeted inhibitors *in vitro*. Associations between genomic alterations and outcomes were analyzed in patients.

[*]**To whom correspondence should be addressed**: Daniel P. Cahill, cahill@mgh.harvard.edu or Andrew S. Chi, chi.andrew@mgh.harvard.edu.

Disclosures: DD, LWE, DRB and AJI have received consultant fees from Bioreference Laboratories; DD, LWE and AJI have a SNaPshot patent pending. MGV has received consultant fees from Agios, honoraria from Boehringer Ingelheim and has equity in Agios and Johnson & Johnson. TTB has received consultant fees from Merck, Roche, Novartis, Champions Biotechnology and Advance Medical and research funding from Pfizer and AstraZeneca. All other authors declare no conflicts.

RESULTS—By 10 months, 8 of 20 *IDH1*-mutant gliomas developed intracerebral xenografts. All xenografts maintained mutant *IDH1* and high levels of 2-hydroxyglutarate on serial transplantation. All xenograft-producing gliomas harbored "lineage-defining" mutations in *CIC* (oligodendroglioma) or *TP53* (astrocytoma), and 6 of 8 additionally had activating mutations in *PIK3CA* or amplification of *PDGFRA*, *MET* or *N-MYC*. Only *IDH1* and *CIC*/*TP53* mutations were detected in non-xenograft-forming gliomas (*P*=.0007). Targeted inhibition of the additional alterations decreased proliferation *in vitro*. Moreover, we detected alterations in known cancer driver genes in 13.4% of *IDH*-mutant glioma patients, including *PIK3CA*, *KRAS*, *AKT* or *PTEN* mutation or *PDGFRA*, *MET* or *N-MYC* amplification. *IDH*/*CIC* mutant tumors were associated with *PIK3CA*/*KRAS* mutations while *IDH*/*TP53* tumors correlated with *PDGFRA*/*MET* amplification. Presence of driver alterations at progression was associated with shorter subsequent progression-free survival (median 9.0 vs. 36.1 months, *P*=.0011).

CONCLUSION—A subset of *IDH*-mutant gliomas with mutations in driver oncogenes has a more malignant phenotype in patients. Identification of these alterations may provide an opportunity for use of targeted therapies in these patients.

Keywords

IDH mutation; glioma; progression; orthotopic xenograft; driver mutation

INTRODUCTION

Shortly after the discovery of recurrent mutations in the isocitrate dehydrogenase (*IDH1*) and *IDH2* genes it was recognized that *IDH*-mutant diffuse gliomas have a clinical phenotype distinct from *IDH*-wildtype gliomas (1-4). More recently, two major genetic subtypes of *IDH*-mutant glioma have been identified: one genetic lineage is defined by *TP53* and alpha thalassemia/mental retardation syndrome x-linked (*ATRX*) mutations and strong correlation with astrocytic histology (1, 2, 5, 6), and a second lineage is characterized by concurrent mutations in homolog of Drosophila capicua (*CIC*), Far Upstream Element Binding Protein (*FUBP1*) and the telomerase reverse transcriptase (*TERT*) promoter as well as tight association with 1p/19q codeletion and oligodendroglioma histopathology (2, 5, 7-12). Notably, the genomic alterations that frequently occur in the more common *IDH*-wildtype primary glioblastoma (GBM, WHO Grade IV), including *EGFR* gene amplification and rearrangement, *PTEN* mutation and *CDKN2A*-*CDKN2B* deletion, are rare in *IDH*-mutant gliomas (2, 5, 12, 13). Thus, *IDH*-mutant gliomas are thought to arise via a molecular pathway that is distinct from primary GBM (5, 6).

Although *IDH*-mutant diffuse gliomas carry a relatively better prognosis (1-4), most ultimately transform to a more malignant phenotype and become lethal. A fundamental paradigm in cancer progression imparts that morphologic changes during the process of malignant transformation reflect the sequential acquisition of genetic alterations (14). *IDH1/2* mutation and widespread hypermethylation of CpG islands (CpG island hypermethylator phenotype or CIMP) are the earliest known events in glioma development, preceding the "lineage-defining" acquisition of *TP53* mutation in astrocytomas or 1p/19q co-deletion in oligodendrogliomas (5, 10, 15-18). Mutant *IDH1/2* represents a "trunk"

mutation (19) in the molecular evolutionary tree of gliomas since it is ubiquitously present throughout the tumor cell mass (15, 20) and retained on progression from low- to high-grade with few exceptions (2, 10, 15, 20, 21). The lineage-defining or "secondary" genetic alterations in *IDH*-mutant gliomas (*TP53*/*ATRX* mutations or 1p/19q codeletion/*CIC* mutations) are also early events in tumor development, as they are present in the vast majority of low-grade (WHO grade II) diffuse gliomas (2, 12). Therefore, "primary" *IDH1/2* mutation and "secondary" genetic alterations are unlikely to be the triggers of more malignant behavior. A few genetic alterations have been reported to be associated with higher grade or progressive *IDH*-mutant gliomas, however the alterations that drive transformation to a more malignant phenotype remain largely unknown (2, 5, 13, 15).

One limitation in the study of *IDH*-mutant glioma has been the scarcity of experimental models harboring endogenous *IDH1/2* mutation. Successful propagation of tumor initiating cells (TICs), cancer cells that display stem cell properties, and generation of intracerebral glioma xenografts from *IDH*-mutant patient gliomas are rare (22-25). The reasons for the difficulty in establishing models from patient *IDH*-mutant gliomas are unknown.

Herein, we hypothesized that additional "tertiary" genetic alterations, which have been noted to occur in *IDH*-mutant gliomas (7, 15, 26, 27), could be the drivers of the progressive malignant phenotype of *IDH*-mutant gliomas. We therefore tested 20 consecutive *IDH*-mutant glioma specimens from patients undergoing surgery at our institution for the ability to establish intracerebral xenografts in mice. We performed a comparative genetic analysis of all primary tumor specimens using a CLIA-certified molecular panel and discovered that the *IDH*-mutant gliomas that successfully established orthotopic xenografts (8 tumors) were enriched with additional tertiary oncogenic genetic alterations, including *PIK3CA* mutation and amplification of the *PDGFRA*, *MET*, and *N-MYC* genes. *IDH*-mutant glioma TICs generated from xenograft-forming tumors exhibit oncogenic addiction to tertiary mutations. In *IDH*-mutant glioma patients, tertiary alterations appear to be acquired at the time of tumor progression and also associated with higher pathological grade and shorter progression-free survival. These data indicate acquisition of tertiary alteration is associated with more aggressive tumor behavior and may predict the ability to establish intracerebral xenografts in mice.

METHODS

Biologic Samples and Clinical Data

From September 2011 to October 2012, we prospectively accrued 20 consecutive untreated (9 patients) and previously treated (11 patients) *IDH*-mutant glioma patients undergoing resection at the Massachusetts General Hospital (MGH). Patients either had previously confirmed *IDH* mutation or were accrued if clinical suspicion of *IDH*-mutant glioma was high based on characteristic features such as young age, frontal location, and lesser degree of contrast enhancement and necrosis on neuroimaging (5). Progression of disease was confirmed by either tissue diagnosis or standard response criteria (28). All tumor samples and clinical information were collected under MGH institutional review board-approved protocols, and informed consent was obtained from all patients. All mouse procedures were approved by the Subcommittee on Research Animal Care at MGH.

Glioma Neurospheres and Orthotopic Xenografts

Fresh surgical specimens were enzymatically dissociated, and 2-5 × 10^4 cells were stereotactically implanted into the right striatum of the brains of 7-10-week-old female SCID mice as described (29). In some cases when an excess of tumor tissue was available, cells were briefly cultured in neurosphere medium as described (30) to enrich for TIC neurospheres, and a similar number of cells were implanted within 48 hours of *in vitro* culture. There was no notable difference in xenograft formation with either method. Mice were monitored for status twice per week and sacrificed when neurological deficits became significant. A minimum 10-month observation period after implantation was required to determine whether orthotopic xenografts developed, although all animals were sacrificed after 1 year to assess for tumor formation. Brains were removed for pathological studies and tumors were excised to re-establish TIC neurosphere cultures. TICs were then either implanted into the brains of new mice or used for *in vitro* assays as described (29, 31).

Histology and Immunostaining

Hematoxylin and eosin staining and immunohistochemistry (IHC) were performed on formalin-fixed paraffin-embedded (FFPE) sections as described (29, 31). Primary antibodies used for IHC were anti-IDH1 R132H (Dianova, 1: 100), Ki-67 (MIB-1, Dako, 1: 150), anti-CD31 (BD Pharmingen, 1: 150) and anti-nestin (Santa Cruz, 1: 400).

Genotyping and Fluorescent in Situ Hybridization Data

Clinical molecular profiling was performed as described (32, 33). Briefly, the MGH SNaPshot assay is a multiplexed, PCR-based, single-base extension assay that interrogates 73 commonly mutated loci from 23 genes (*AKT1*, *APC*, *BRAF*, *CTNNB1*, *EGFR*, *EML4-ALK*, *HER2*, *FGFR3*, *GNA11*, *GNAQ*, *GNAS*, *HRAS*, *IDH1*, *IDH2*, *KIT*, *KRAS*, *MEK1*, *NOTCH1*, *NRAS*, *PIK3CA*, *PTEN*, *RET*, *TP53*). Genomic PCR-based sequencing was used to sequence all coding exons of the *IDH1*, *CIC*, *TP53*, *PIK3CA* and *PIK3R1* genes. PCR products were amplified from genomic DNA templates with Platinum Taq polymerase per manufacturer's protocol using intron-based primers spanning the expressed coding sequences (**Supplementary Table S2**) then Sanger sequenced (Beckman Coulter Genomics). Fluorescence in situ hybridization (FISH) assays for the *EGFR*, *MET* and *PDGFRA g*enes were performed using BAC probes CTD-2113A18 (7p *EGFR* locus), CTB-13N12 (7q *MET* locus), CEP7 (centromere 7 control), RP11-58C6 (4q *PDGFRA* locus) and CEP4 (centromere 4 control) (Abbott) as described (32). BAC clone RP11-480N14 (chr2: 15991148-16158895) was used to make the *N-MYC* probe and ALK (2p23) Proximal Probe (Kreatech) was used for centromere 2 control. Gene/control probe copy number ratios of >2.0 were considered amplified. 1p and 19q status was determined using the Vysis 1p36/1q25 and 19q13/19p13 FISH Probe Kit (Abbott). 1p/1q and 19q/19p ratios of <0.75 were considered loss and >0.75 as maintained.

Gas chromatography-mass spectroscopy (GC-MS) Data

Ten to 20 mg of frozen tumor tissue was homogenized and extracted with methanol/ chloroform. Metabolites were derivatized with N-(tert-butyldimethylsilyl)-N- methyl-trifluoroacetamide, with 1% tert-Butyldimethylchlorosilane (Sigma) and analyzed on a

6890N GC system (Agilent Technologies) combined with a 5975B Inert XL MS system (Agilent Technologies). 2HG fragment 433m/z and the glutamate fragment 432m/z were used for further analysis (34). 2HG and glutamate concentrations were normalized to the internal standard norvaline and tissue weight as described (35).

In vitro Drug and shRNA Inhibition Studies

Dissociated TICs were seeded to 96-well plates at 7000 - 8000 cells per well. Serially diluted inhibitor was added to wells, and cells were further cultured for 5 days. Viability of cells was measured by CellTiter-Glo assay (Promega) and the EC50 values were determined. All *in vitro* inhibitor assays were performed on TICs within 5 passages from dissociation from tumor. JQ1 and BYL719 were gifts from James E. Bradner and Jeffrey A. Engelman, respectively. Crizotinib and sunitinib were obtained from Selleck Chemicals.

To knock down N-myc expression, lentivirus vectors carrying shRNA for *N-MYC* (Sigma, pLKO.1) were packaged using ScreenFect (Wako)-mediated co-transfection of vector and packaging plasmid DNAs to 293T cells. MGG152 cells were infected with lentivirus in the presence of polybrene (6 μg/ml), selected with puromycin (0.5 μg/ml) for 3 days, and silencing confirmed with Western blot. Cell viability and sphere formation were assessed 7 days later.

Statistical Analyses

Statistical analysis was performed with JMP software. For parametric analyses, two-tailed t-tests were employed and for analysis of frequencies of nominal data, two-tailed Fisher's Exact test was employed. Data are expressed as mean + SD. Survival was analyzed by the Kaplan-Meier method with two-sided log-rank statistics.

RESULTS

Establishment of Intracerebral Xenografts with Endogenous *IDH* Mutation

We studied the potential of 20 serially collected patient *IDH1*-mutant glioma specimens to form xenograft after stereotactic implantation in immunocompromised mouse brains. Two tumors were low-grade (WHO grade II), 10 were anaplastic (WHO grade III), and 8 were GBMs, of which 3 were “secondary” GBMs that had transformed from a known lower-grade glioma (**Table 1**). All 20 gliomas in our study had *IDH1* mutations, which occur far more frequently than *IDH2* mutations in gliomas (2, 36). In parallel, we cultured TIC-enriched cells using the neurosphere system. Notably, 8 of 20 *IDH*-mutant glioma tumors generated intracerebral xenografts, with the time to lethal xenograft ranging between 1-7 months (**Fig. 1, Table 1, Supplementary Fig. S1**). All xenografts closely recapitulated parent human tumor phenotypes histologically (**Fig. 1, Supplementary Figs. S1, S2, S3, Table 1**). *In vitro* proliferation of the different lines varied, with doubling times ranging from 2.5 days (MGG152) to 10 days (MGG79, MGG108, MGG132). All lines could be passaged for at least 5 passages, however 2 lines (MGG119, MGG152) could be stably cultured for at least 4 months. All xenografts harbored endogenous *IDH1 R132H* mutation and retained the mutant allele upon serial passage *in vitro* or serial transplantation in orthotopic xenograft (**Supplementary Figs. S4, S5)**. Orthotopic xenografts were confirmed

by GC-MS to have high-level production of the mutant-specific metabolite, 2-hydroxyglutarate (2HG) (**Supplementary Table S1**).

Genetic Alterations Associated With Ability to Generate Intracerebral Xenograft

We sought to identify the mechanisms accounting for the ability to generate orthotopic xenograft in our set of *IDH*-mutant gliomas. There was no clear distinction in host factors such as patient age, sex, or prior treatment (radiation or various combinations of radiation and different chemotherapies; **Table 1**) between gliomas that formed orthotopic xenograft versus those that did not. Generally, tumors that were able to form xenografts had GBM (WHO grade IV) histology (6 of 8 xenografts vs. 2 of 12 in the non-xenograft-forming subset) and lacked 1p/19q codeletion (7 of 8 xenografts).

We conducted a comparative genetic analysis on the primary tumor specimens to assess whether additional oncogenic alterations might account for differences in the ability to generate xenograft. All 8 xenograft-forming tumors and 10 of 12 non-xenograft-forming tumors harbored the *IDH1 R132H* variant, which accounts for ~90% of the *IDH1* mutations in gliomas (2, 12, 36), and the remaining two non-xenograft-forming gliomas harbored *IDH1 R132C*. Interestingly, one glioma xenograft (MGG79) was homozygous for *IDH1 R132H* mutation and the corresponding orthotopic xenograft produced high-levels of 2HG (**Supplementary Fig. S4, Supplementary Table S1**). This finding is in contrast with a previous report suggesting a wild-type *IDH1* allele is necessary for 2HG production (37).

Focused genotyping analysis of all implanted primary tumors was conducted with our CLIA-certified clinical molecular profiling platform (32), which surveys 25 commonly-mutated cancer-associated genes. We specifically assessed for “tertiary” genetic alterations, which we defined as non-lineage mutations, since lineage-associated mutations (astrocytic *ATRX*/*TP53* mutations or oligodendroglial *CIC*/*TERT* mutations and 1p/19q codeletion) occur in virtually all low-grade *IDH*-mutant gliomas. Strikingly, 6 of 8 xenograft-forming tumors harbored tertiary mutations whereas none were detected in non-xenograft-forming patient gliomas ($P = .0007$) (**Table 1**).

The detected tertiary alterations included hotspot activating mutations in *PIK3CA* (2/6) and high-level focal amplifications in the *PDGFRA* (2/6) and *MET* (1/6) genes (**Table 1**). In addition, we sequenced the entire coding regions of *PIK3CA*, which encodes p110alpha, and *PIK3R1*, which encodes the PI3K regulatory subunit p85alpha, in all xenograft-forming tumors and detected no other mutations. Notably, one GBM had focal primitive neuroectodermal tumor (PNET) histopathology (MGG152, **Fig. 1A**) and was unusually malignant in both the patient (5 month overall survival) and in orthotopic xenograft (lethal within 1 month, **Table 1**). A previous study detected *C-MYC* or *N-MYC* amplification in a significant proportion of malignant gliomas harboring PNET-like components (38), therefore we interrogated these genes in MGG152 and identified high-level *N-MYC* amplification (**Fig. 2A**). We confirmed that all the tertiary genetic alterations detected in the primary tumors were maintained in the respective orthotopic xenografts (**Fig. 2A**), suggesting these mutations play a role in the tumor initiating capability of *IDH1*-mutant gliomas.

Tertiary Genetic Alterations are Drivers in *IDH*-Mutant Glioma Xenografts

We then tested the effect of small molecule inhibitors targeted at the identified tertiary mutations on *in vitro* proliferation. We examined the impact of BYL719, a highly selective inhibitor of p110alpha (39), on the viability of MGG108 (*PIK3CA* R93Q) and MGG152 (*PIK3CA*/*PIK3R1* wildtype) TICs. We observed more potent inhibition of MGG108 than MGG152 cells (IC_{50} = 7.5 μM for MGG108 vs. 20.1 μM for MGG152), indicating *PIK3CA* mutation functions as a driver of proliferation in MGG108 cells (**Fig. 2B)**. We then examined the effect of the Myc pathway small molecule inhibitor JQ1 (40) in MGG108 and MGG152 (*N-MYC* amplified). As expected, MGG152 was significantly more sensitive to JQ1 in cell viability assays relative to MGG108, which lacks *N-MYC* or *C-MYC* amplification (IC_{50} = 0.04 μM for MGG152 vs. 2.08 μM for MGG108) (**Fig. 2B**). Furthermore, shRNA knockdown of N-myc expression in MGG152 suppressed cell proliferation and nearly eliminated sphere formation ability (**Fig. 2C, Supplementary Fig. S6**). We also tested sunitinib and crizotinib, small molecule inhibitors of PDGFR and c-Met, respectively, in several lines with known *PDGFRA* and *MET* copy number status. We found that sunitinib was more potent against a line with high-level *PDGFRA* amplification (MGG117) than those without (MGG108 and MGG119), while crizotinib was most effective in a line harboring *MET* amplification (MGG132) (**Supplementary Fig. S7).** These data suggest that tertiary alterations are oncogenic drivers in *IDH*-mutant glioma xenografts.

Acquisition of Tertiary Mutations During Malignant Transformation

We then asked whether tertiary alterations are acquired when lower-grade *IDH*-mutant gliomas progress or transform to higher grade tumors in patients. We examined our dataset of 149 *IDH*-mutant glioma patients who had clinical molecular profiling at our center and identified 20 tumors with tertiary alterations (13.4%). Tertiary alterations were nearly exclusively present in progressive low-grade (WHO grade II) or high-grade (WHO grade III or IV) tumors (**Table 2**); specifically 6 grade II (4 progressive), 6 grade III and 8 grade IV tumors. Presence of a tertiary mutation was associated with grade IV (GBM) vs. lower grade (grade II or III) histology (*P* = .027).

We then analyzed a subset of 56 patients who underwent biopsy and genotyping at the time of radiographically defined disease progression. Presence of tertiary alteration in the progressive tumor (14 patients, 25%) was associated with significantly shorter subsequent PFS (median 9.0 months, 95% CI 4.4 - 49.3, with tertiary alteration versus 36.1 months, 95% CI 18.7 - 52.8, without (*P* = .0011) (**Figs. 3A, 3B**). Notably, there was no difference in PFS from the time of initial diagnosis (median 55.6 months, 95% CI 24.6- 93.1, with tertiary alteration versus 54.1 months, 95% CI 35.7 - 73.0, without, *P* = .76) (**Fig. 3A**), implicating the tertiary alteration detected at progression as the driver of malignant degeneration in these patients. There was no detectable difference in overall survival, however there were few deaths in either group (13 of 56 total patients) therefore longer follow-up time is needed to assess this endpoint.

Several tertiary genetic events were recurrently identified (**Table 2**), including activating mutations in *PIK3CA* (9 tumors) and *KRAS* (4 tumors) and *PDGFRA* amplification (4

tumors). *PIK3CA* and *KRAS* mutations were most often detected in tumors with at least a component of oligodendroglioma histology (7 of 9 *PIK3CA* mutant and 3 of 4 *KRAS* mutant tumors). Interestingly, all 4 *PDGFRA*-amplified tumors were purely astrocytic ($P = .026$). When specific oncogenes were compared by *IDH* genetic lineage rather than histopathology (within the set of tumors with tertiary mutations and confirmed lineage mutations), we identified significant associations between 1p/19q codeleted tumors and intracellular signaling pathway gene mutations (*KRAS* or *PIK3CA*, $P = .002$) and between receptor tyrosine kinase amplification (*PDGFRA* or *MET*) and non-1p/19q codeleted (*TP53* mutant) tumors ($P = .029$).

To assess whether tertiary alterations are acquired at tumor progression, we examined paired tumor specimens from newly diagnosed and progressive tumors from 6 patients in whom we detected tertiary mutations. For two patients with *PDGFRA* amplification and one patient with focal *MET* amplification, we confirmed these alterations were present in the progressive but not in the initial tumor specimens (**Fig. 3C**). In 2 of 3 *PIK3CA* mutant patients, the *PIK3CA* mutations were present only in the progressive tumor (**Fig. 3C**). The third patient (Patient 6 in Table 2) had *PIK3CA E545G* mutation in both the diagnostic and progressive tumor specimens. This patient was treated with 12 cycles of temozolomide and progressed just 24.6 months after diagnosis, a relatively rapid time to progression for low-grade oligodendrogliomas with 1p/19q codeletion.

DISCUSSION

IDH-mutant diffuse gliomas nearly always progress after radiation therapy and chemotherapy and eventually transform to more malignant tumors. Effective therapeutic options at that stage are lacking. Herein we demonstrate that the subset of *IDH*-mutant gliomas that acquire an aggressive phenotype late in the disease are driven by specific tertiary oncogenic alterations. These tertiary alterations are associated with more malignant tumors in patients and increased tumor-forming ability in mice. Importantly, these tertiary alterations represent potential therapeutic targets for patients with *IDH*-mutant gliomas who are most in need of treatment.

Our data suggest that after acquisition of lineage-defining mutations, *IDH*-mutant gliomas may follow multiple pathways to transformation (**Fig. 4**). 1p/19q codeleted tumors tend to activate the PI3K/mTOR or Ras intracellular signaling pathways and *TP53*-mutant tumors tend to amplify growth factor receptor tyrosine kinases. Our findings are consistent with prior reports; recurrent *PIK3CA* mutations have been detected in a subset of *IDH*-mutant, 1p/19q codeleted anaplastic oligodendrogliomas (7, 26) and two recent reports observed enrichment of *PDGFRA* amplification in *IDH*-mutant versus *IDH*-wildtype primary GBM (27, 41). In addition, we find that activation of N-myc may be a particularly malignant transformation pathway in *IDH*-mutant glioma. A recent study similarly observed a correlation between c-Myc expression and shorter time to transformation within *IDH*-mutant gliomas (42). Together with these reports, our data suggests *IDH*-mutant gliomas may undergo a sequenced genetic evolution analogous to *IDH2*-mutant acute myeloid leukemia, where stepwise acquisition of distinct classes of mutations results in more aggressive disease (43).

The mechanisms by which *IDH*-mutant gliomas acquire tertiary mutations are largely unknown. A recent study observed that a subset of *IDH*-mutant low-grade gliomas developed a hypermutation phenotype (15, 44) after treatment with temozolomide. All of the hypermutated gliomas in their dataset harbored driver mutations, many in the PI3K/mTOR signaling pathway (15). In our dataset, 10 of 20 patients with tertiary mutation were previously treated with alkylating chemotherapy (**Table 2**). Five of our 10 chemotherapy-treated patients had PI3K/mTOR pathway mutations in their tumors, and interestingly one tumor had activating mutations in 3 oncogenes (*PIK3CA*, *AKT* and *KRAS*), suggesting it may be hypermutated. However, 9 patients as well as two xenograft-forming tumors from our implantation study harbored tertiary alterations and had no prior treatment, indicating that genomic instability resulting from DNA-damaging therapy is not the sole evolutionary path to malignant progression in *IDH*-mutant gliomas. The drivers of tertiary mutation in untreated *IDH*-mutant tumors remain to be determined.

The overall frequency of tertiary mutations in our dataset was 13.4%, which may be reflective of the focused nature of our genotyping panel. Our data suggests re-sampling of tumor specimens at the time of progression may increase detection frequencies. We also provide rationale for sampling tumor specimens throughout the course of disease as the acquired tertiary mutation may present an opportunity for therapeutic targeting. Future genomic profiling studies that also include paired tumor samples will address important remaining questions including the scope and frequency of recurrent tertiary mutations, the timing of their appearance and the mechanisms that drive their development. Of note, our genotyping panel did not interrogate many genes commonly mutated in gliomas, such as *CDK4/6*, *MDM2*, *CCND2*, *AKT3*, *RB*, *PARK2* and *NF1* (1, 45). However, these mutations were detected in datasets consisting mostly of *IDH*-wildtype gliomas that evolve along a distinct molecular pathway.

By identifying recurrent, functionally significant tertiary genetic alterations, we set the stage for targeted therapy in *IDH*-mutant gliomas. Pharmacologic inhibitors for all of the tertiary alterations identified in our work are in development. Notably, our data suggests *PDGFRA* amplification warrants investigation in *TP53*-mutant, *IDH*-mutant gliomas. Outcomes for this subgroup are poor relative to the 1p/19q codeleted subtype (6) possibly due to the uncertain efficacy of chemotherapy in these tumors given their lack of 1p/19q codeletion (46, 47). We detected recurrent mutations in *KRAS*, which have been reported to be rare in glial tumors (45, 48, 49). Recent clinical data suggest that cancers driven by *KRAS* mutation may be sensitive to MEK inhibitors (50). Additionally, our data suggests investigation of Myc pathway inhibitors (40) may be justified for particularly aggressive *IDH*-mutant gliomas, since these may harbor C-*MYC* or *N-MYC* amplification or inappropriate c-Myc expression. Analogously, a recent study reported that Myc pathway inhibition potently reduces viability of acute myeloid leukemia cells driven by mutant *IDH2* (43).

Finally, development of anticancer agents in *IDH*-mutant gliomas has been limited by the scarcity of biologically accurate preclinical models that are serviceable for testing therapeutics. We have established a panel of endogenous *IDH*-mutant intracerebral glioma xenografts that represent a powerful platform for studying *IDH*-mutant tumor biology and for answering fundamental questions regarding treatment of *IDH*-mutant gliomas. Future

work utilizing these orthotopic xenografts may help determine the optimal therapeutic strategy for *IDH*-mutant gliomas, which may involve inhibition of mutant *IDH1*, inhibition of tertiary genetic alterations, alteration of metabolic or epigenetic pathways, or a combination thereof.

Supplementary Material

Refer to Web version on PubMed Central for supplementary material.

Acknowledgments

We thank Alona Muzikansky for assistance with the biostatistical analysis.

Financial Support: American Cancer Society Institutional Research Grant and Richard B. Simches Scholars Award (ASC), Burroughs-Wellcome Career Award (DPC).

REFERENCES

1. Parsons D, Jones S, Zhang X, Lin J, Leary R, Angenendt P, et al. An integrated genomic analysis of human glioblastoma multiforme. Science. 2008; 321:1807–12. [PubMed: 18772396]
2. Yan H, Parsons D, Jin G, McLendon R, Rasheed B, Yuan W, et al. IDH1 and IDH2 mutations in gliomas. N Engl J Med. 2009; 360:765–73. [PubMed: 19228619]
3. Houillier C, Wang X, Kaloshi G, Mokhtari K, Guillevin R, Laffaire J, et al. IDH1 or IDH2 mutations predict longer survival and response to temozolomide in low-grade gliomas. Neurology. 2010; 75:1560–6. [PubMed: 20975057]
4. Hartmann C, Hentschel B, Wick W, Capper D, Felsberg J, Simon M, et al. Patients with IDH1 wild type anaplastic astrocytomas exhibit worse prognosis than IDH1-mutated glioblastomas, and IDH1 mutation status accounts for the unfavorable prognostic effect of higher age: implications for classification of gliomas. Acta Neuropathol. 2010; 120:707–18. [PubMed: 21088844]
5. Lai A, Kharbanda S, Pope WB, Tran A, Solis OE, Peale F, et al. Evidence for Sequenced Molecular Evolution of IDH1 Mutant Glioblastoma From a Distinct Cell of Origin. J Clin Oncol. 2011; 29:4482–90. [PubMed: 22025148]
6. Jiao Y, Killela PJ, Reitman ZJ, Rasheed AB, Heaphy CM, de Wilde RF, et al. Frequent ATRX, CIC, and FUBP1 mutations refine the classification of malignant gliomas. Oncotarget. 2012; 3:709–22. [PubMed: 22869205]
7. Bettegowda C, Agrawal N, Jiao Y, Sausen M, Wood LD, Hruban RH, et al. Mutations in CIC and FUBP1 contribute to human oligodendroglioma. Science. 2011; 333:1453–5. [PubMed: 21817013]
8. Yip S, Butterfield YS, Morozova O, Chittaranjan S, Blough MD, An J, et al. Concurrent CIC mutations, IDH mutations, and 1p/19q loss distinguish oligodendrogliomas from other cancers. J Pathol. 2012; 226:7–16. [PubMed: 22072542]
9. Killela PJ, Reitman ZJ, Jiao Y, Bettegowda C, Agrawal N, Diaz LA Jr. et al. TERT promoter mutations occur frequently in gliomas and a subset of tumors derived from cells with low rates of self-renewal. Proc Natl Acad Sci U S A. 2013; 110:6021–6. [PubMed: 23530248]
10. Watanabe T, Nobusawa S, Kleihues P, Ohgaki H. IDH1 mutations are early events in the development of astrocytomas and oligodendrogliomas. Am J Pathol. 2009; 174:1149–53. [PubMed: 19246647]
11. Ichimura K, Pearson DM, Kocialkowski S, Backlund LM, Chan R, Jones DT, et al. IDH1 mutations are present in the majority of common adult gliomas but rare in primary glioblastomas. Neuro Oncol. 2009; 11:341–7. [PubMed: 19435942]
12. Balss J, Meyer J, Mueller W, Korshunov A, Hartmann C, von Deimling A. Analysis of the IDH1 codon 132 mutation in brain tumors. Acta Neuropathol. 2008; 116:597–602. [PubMed: 18985363]

13. Nobusawa S, Watanabe T, Kleihues P, Ohgaki H. IDH1 mutations as molecular signature and predictive factor of secondary glioblastomas. Clin Cancer Res. 2009; 15:6002–7. [PubMed: 19755387]
14. Vogelstein B, Kinzler KW. The multistep nature of cancer. Trends Genet. 1993; 9:138–41. [PubMed: 8516849]
15. Johnson BE, Mazor T, Hong C, Barnes M, Aihara K, McLean CY, et al. Mutational analysis reveals the origin and therapy-driven evolution of recurrent glioma. Science. 2014; 343:189–93. [PubMed: 24336570]
16. Turcan S, Rohle D, Goenka A, Walsh LA, Fang F, Yilmaz E, et al. IDH1 mutation is sufficient to establish the glioma hypermethylator phenotype. Nature. 2012
17. Kannan K, Inagaki A, Silber J, Gorovets D, Zhang J, Kastenhuber ER, et al. Whole-exome sequencing identifies ATRX mutation as a key molecular determinant in lower-grade glioma. Oncotarget. 2012; 3:1194–203. [PubMed: 23104868]
18. Yan H, Bigner DD, Velculescu V, Parsons DW. Mutant metabolic enzymes are at the origin of gliomas. Cancer Res. 2009; 69:9157–9. [PubMed: 19996293]
19. Gerlinger M, Rowan AJ, Horswell S, Larkin J, Endesfelder D, Gronroos E, et al. Intratumor heterogeneity and branched evolution revealed by multiregion sequencing. N Engl J Med. 2012; 366:883–92. [PubMed: 22397650]
20. Capper D, Weissert S, Balss J, Habel A, Meyer J, Jager D, et al. Characterization of R132H mutation-specific IDH1 antibody binding in brain tumors. Brain Pathol. 2010; 20:245–54. [PubMed: 19903171]
21. Walker EJ, Zhang C, Castelo-Branco P, Hawkins C, Wilson W, Zhukova N, et al. Monoallelic expression determines oncogenic progression and outcome in benign and malignant brain tumors. Cancer Res. 2012; 72:636–44. [PubMed: 22144470]
22. Klink B, Miletic H, Stieber D, Huszthy PC, Valenzuela JA, Balss J, et al. A novel, diffusely infiltrative xenograft model of human anaplastic oligodendroglioma with mutations in FUBP1, CIC, and IDH1. PLoS ONE. 2013; 8:e59773. [PubMed: 23527265]
23. Joo KM, Kim J, Jin J, Kim M, Seol HJ, Muradov J, et al. Patient-specific orthotopic glioblastoma xenograft models recapitulate the histopathology and biology of human glioblastomas in situ. Cell Rep. 2013; 3:260–73. [PubMed: 23333277]
24. Luchman HA, Stechishin OD, Dang NH, Blough MD, Chesnelong C, Kelly JJ, et al. An in vivo patient-derived model of endogenous IDH1-mutant glioma. Neuro Oncol. 2011
25. Kelly JJ, Blough MD, Stechishin OD, Chan JA, Beauchamp D, Perizzolo M, et al. Oligodendroglioma cell lines containing t(1;19)(q10;p10). Neuro Oncol. 2010; 12:745–55. [PubMed: 20388696]
26. Broderick DK, Di C, Parrett TJ, Samuels YR, Cummins JM, McLendon RE, et al. Mutations of PIK3CA in anaplastic oligodendrogliomas, high-grade astrocytomas, and medulloblastomas. Cancer Res. 2004; 64:5048–50. [PubMed: 15289301]
27. Phillips JJ, Aranda D, Ellison DW, Judkins AR, Croul SE, Brat DJ, et al. PDGFRA Amplification is Common in Pediatric and Adult High-Grade Astrocytomas and Identifies a Poor Prognostic Group in IDH1 Mutant Glioblastoma. Brain Pathol. 2013; 23:565–73. [PubMed: 23438035]
28. Wen PY, Macdonald DR, Reardon DA, Cloughesy TF, Sorensen AG, Galanis E, et al. Updated response assessment criteria for high-grade gliomas: response assessment in neuro-oncology working group. J Clin Oncol. 2010; 28:1963–72. [PubMed: 20231676]
29. Wakimoto H, Kesari S, Farrell C, Curry WJ, Zaupa C, Aghi M, et al. Human glioblastoma-derived cancer stem cells: establishment of invasive glioma models and treatment with oncolytic herpes simplex virus vectors. Cancer Res. 2009; 69:3472–81. [PubMed: 19351838]
30. Yuan X, Curtin J, Xiong Y, Liu G, Waschsmann-Hogiu S, Farkas D, et al. Isolation of cancer stem cells from adult glioblastoma multiforme. Oncogene. 2004; 23:9392–400. [PubMed: 15558011]
31. Wakimoto H, Mohapatra G, Kanai R, Curry WT Jr. Yip S, Nitta M, et al. Maintenance of primary tumor phenotype and genotype in glioblastoma stem cells. Neuro Oncol. 2012; 14:132–44. [PubMed: 22067563]

32. Chi AS, Batchelor TT, Dias-Santagata D, Borger D, Stiles CD, Wang DL, et al. Prospective, high-throughput molecular profiling of human gliomas. J Neurooncol. 2012; 110:89–98. [PubMed: 22821383]
33. Dias-Santagata D, Akhavanfard S, David SS, Vernovsky K, Kuhlmann G, Boisvert SL, et al. Rapid targeted mutational analysis of human tumours: a clinical platform to guide personalized cancer medicine. EMBO Mol Med. 2010; 2:146–58. [PubMed: 20432502]
34. Fendt SM, Bell EL, Keibler MA, Olenchock BA, Mayers JR, Wasylenko TM, et al. Reductive glutamine metabolism is a function of the alpha-ketoglutarate to citrate ratio in cells. Nat Commun. 2013; 4:2236. [PubMed: 23900562]
35. Fendt SM, Bell EL, Keibler MA, Davidson SM, Wirth GJ, Fiske B, et al. Metformin decreases glucose oxidation and increases the dependency of prostate cancer cells on reductive glutamine metabolism. Cancer Res. 2013; 73:4429–38. [PubMed: 23687346]
36. Hartmann C, Meyer J, Balss J, Capper D, Mueller W, Christians A, et al. Type and frequency of IDH1 and IDH2 mutations are related to astrocytic and oligodendroglial differentiation and age: a study of 1,010 diffuse gliomas. Acta Neuropathol. 2009; 118:469–74. [PubMed: 19554337]
37. Jin G, Reitman ZJ, Duncan CG, Spasojevic I, Gooden DM, Rasheed BA, et al. Disruption of wild-type IDH1 suppresses D-2-hydroxyglutarate production in IDH1-mutated gliomas. Cancer Res. 2013; 73:496–501. [PubMed: 23204232]
38. Perry A, Miller CR, Gujrati M, Scheithauer BW, Zambrano SC, Jost SC, et al. Malignant gliomas with primitive neuroectodermal tumor-like components: a clinicopathologic and genetic study of 53 cases. Brain Pathol. 2009; 19:81–90. [PubMed: 18452568]
39. Furet P, Guagnano V, Fairhurst RA, Imbach-Weese P, Bruce I, Knapp M, et al. Discovery of NVP-BYL719 a potent and selective phosphatidylinositol-3 kinase alpha inhibitor selected for clinical evaluation. Bioorg Med Chem Lett. 2013; 23:3741–8. [PubMed: 23726034]
40. Delmore JE, Issa GC, Lemieux ME, Rahl PB, Shi J, Jacobs HM, et al. BET bromodomain inhibition as a therapeutic strategy to target c-Myc. Cell. 2011; 146:904–17. [PubMed: 21889194]
41. Burford A, Little SE, Jury A, Popov S, Laxton R, Doey L, et al. Distinct phenotypic differences associated with differential amplification of receptor tyrosine kinase genes at 4q12 in glioblastoma. PLoS ONE. 2013; 8:e71777. [PubMed: 23990986]
42. Odia Y, Orr BA, Robert Bell W, Eberhart CG, Rodriguez FJ. cMYC expression in infiltrating gliomas: associations with IDH1 mutations, clinicopathologic features and outcome. J Neurooncol. 2013 Epub Aug 11.
43. Chen C, Liu Y, Lu C, Cross JR, Morris JPt, Shroff AS, et al. Cancer-associated IDH2 mutants drive an acute myeloid leukemia that is susceptible to Brd4 inhibition. Genes Dev. 2013; 27:1974–85. [PubMed: 24065765]
44. Hunter C, Smith R, Cahill D, Stephens P, Stevens C, Teague J, et al. A hypermutation phenotype and somatic MSH6 mutations in recurrent human malignant gliomas after alkylator chemotherapy. Cancer Res. 2006; 66:3987–91. [PubMed: 16618716]
45. Cancer Genome Atlas Research Network. Comprehensive genomic characterization defines human glioblastoma genes and core pathways. Nature. 2008; 455:1061–8. [PubMed: 18772890]
46. van den Bent MJ, Brandes AA, Taphoorn MJ, Kros JM, Kouwenhoven MC, Delattre JY, et al. Adjuvant procarbazine, lomustine, and vincristine chemotherapy in newly diagnosed anaplastic oligodendroglioma: long-term follow-up of EORTC brain tumor group study 26951. J Clin Oncol. 2013; 31:344–50. [PubMed: 23071237]
47. Cairncross G, Wang M, Shaw E, Jenkins R, Brachman D, Buckner J, et al. Phase III trial of chemoradiotherapy for anaplastic oligodendroglioma: long-term results of RTOG 9402. J Clin Oncol. 2013; 31:337–43. [PubMed: 23071247]
48. Knobbe CB, Reifenberger J, Reifenberger G. Mutation analysis of the Ras pathway genes NRAS, HRAS, KRAS and BRAF in glioblastomas. Acta Neuropathol. 2004; 108:467–70. [PubMed: 15517309]
49. Jeuken J, van den Broecke C, Gijsen S, Boots-Sprenger S, Wesseling P. RAS/RAF pathway activation in gliomas: the result of copy number gains rather than activating mutations. Acta Neuropathol. 2007; 114:121–33. [PubMed: 17588166]

50. Janne PA, Shaw AT, Pereira JR, Jeannin G, Vansteenkiste J, Barrios C, et al. Selumetinib plus docetaxel for KRAS-mutant advanced non-small-cell lung cancer: a randomised, multicentre, placebo-controlled, phase 2 study. Lancet Oncol. 2013; 14:38–47. [PubMed: 23200175]

Statement of Translational Relevance

Recurrent mutations in the isocitrate dehydrogenase 1 (*IDH1*) and *IDH2* genes identify gliomas with a better prognosis. However, most *IDH*-mutant gliomas eventually transform to more aggressive tumors and become fatal. The genetic events that drive this later malignant behavior are largely unknown. Here, we find that a subset of *IDH*-mutant gliomas acquire mutations in cancer driver genes when they recur. Presence of these mutations is associated with more rapid subsequent progression. We also find that genetic subtypes of *IDH*-mutant gliomas utilize distinct oncogenic pathways during transformation to more malignant tumors. Moreover, *IDH*-mutant gliomas with driver mutations preferentially establish orthotopic xenograft tumors in mouse brain and are sensitive to targeted inhibition of the mutant gene product. Identification of targetable recurrent driver mutations provides novel therapeutic possibilities for the *IDH*-mutant glioma patients who are most in need of new treatments.

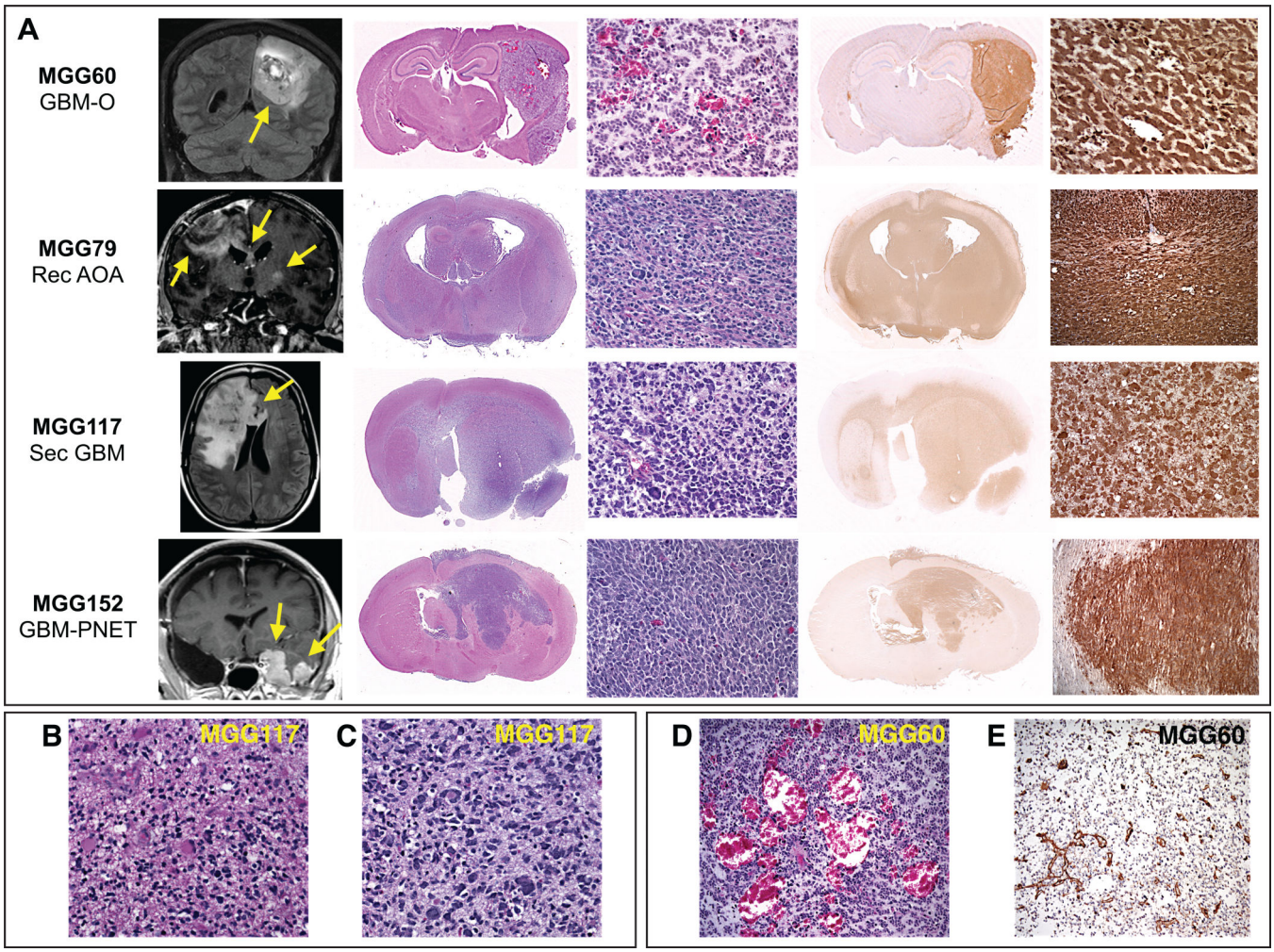

Figure 1. Mouse orthotopic xenografts generated from patient *IDH1* R132H-mutant gliomas

(A) Rows: Individual *IDH1*-mutant glioma orthotopic (intracerebral) xenografts. Columns left to right: xenograft line and patient tumor histology; representative patient MRI (yellow arrows highlight areas of tumor); gross xenograft histological hematoxylin and eosin (HE) section; microscopic xenograft HE section; gross xenograft immunohistochemical (IHC) section stained with IDH1 R132H mutant-specific antibody (brown); microscopic xenograft anti-IDH1 R132H (brown) IHC. Predominantly nodular (MGG60, 152) and infiltrative (MGG79, 117) growth patterns of xenografts are in accordance with the respective human tumors as demonstrated by MRI. (B and C) Microscopic section of MGG117 primary tumor (B) and orthotopic xenograft (C) showing marked cellular heterogeneity and nuclear pleomorphism in both sections. (D and E) MGG60 xenograft demonstrating tumor angiogenesis by (D) HE and (E) endothelium-specific anti-CD31 antibody IHC. GBM-O, GBM with oligodendroglial component; Rec AOA, recurrent anaplastic oligoastrocytoma; Sec GBM, secondary GBM; GBM-PNET, GBM with primitive neuroectodermal tumor component.

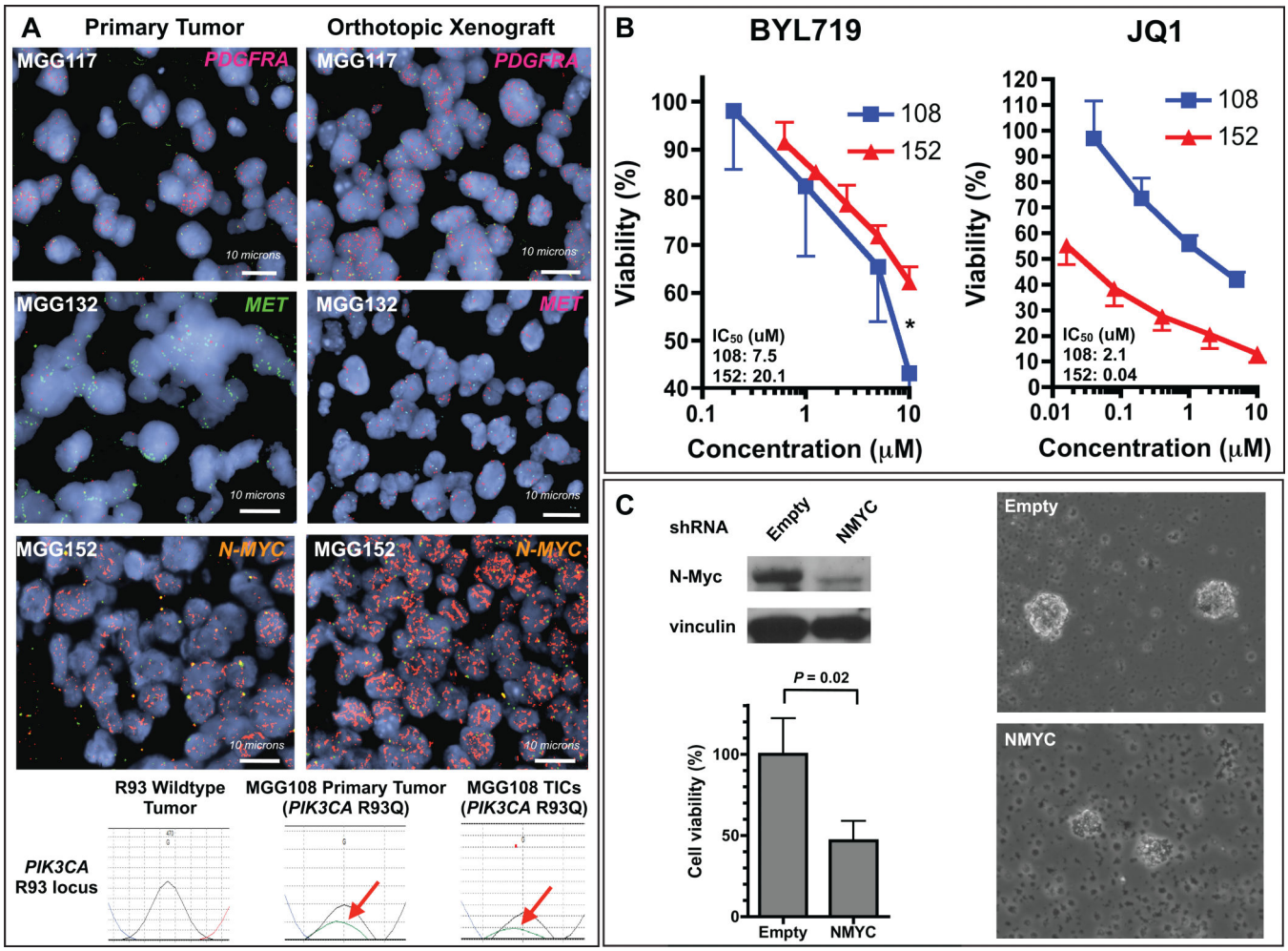

Figure 2. Recurrent tertiary genetic alterations in *IDH*-mutant gliomas drive tumor cell growth

(A) Fluorescent in situ hybridization (FISH) images of primary tumors (left column) and corresponding orthotopic xenografts (right column). Top row: MGG117 probed with *PDGFRA* (red) and CEN4 control (green). 2nd row: MGG132 primary tumor (left) probed with *MET* (green) and CEN7 control (red) and xenograft (right) probed with *MET* (red) and CEN7 (green). 3rd row: MGG152 probed with *N-MYC* (orange) and 2p23 control (green). Bottom row: Sequencing traces of the *PIK3CA* R93 locus with wildtype (black trace) and mutant (green trace, red arrow) alleles. Left: *PIK3CA* wildtype primary tumor (control). Middle: MGG108 primary tumor. Right: MGG108 TICs. (B) Effect of BYL719 and JQ1 on MGG108 and MGG152 TICs. Asterisk: MGG108 (*PIK3CA* mutant) and MGG152 (*N-MYC* amplified) at 10 μM of BYL719 (P = .004, t-test). (C) N-Myc knockdown in MGG152 TICs. MGG152 was infected with lentivirus carrying *N-MYC* shRNA or empty vector. Upper left panel: Western blot of TICs using antibodies against N-myc and vinculin (loading control). Lower left panel: Cell viability assays of TICs expressing *N-MYC* shRNA or empty vector. Right panels: TIC neurospheres infected with lentivirus carrying empty (upper) or *N-MYC* shRNA (lower). TIC, tumor initiating cell.

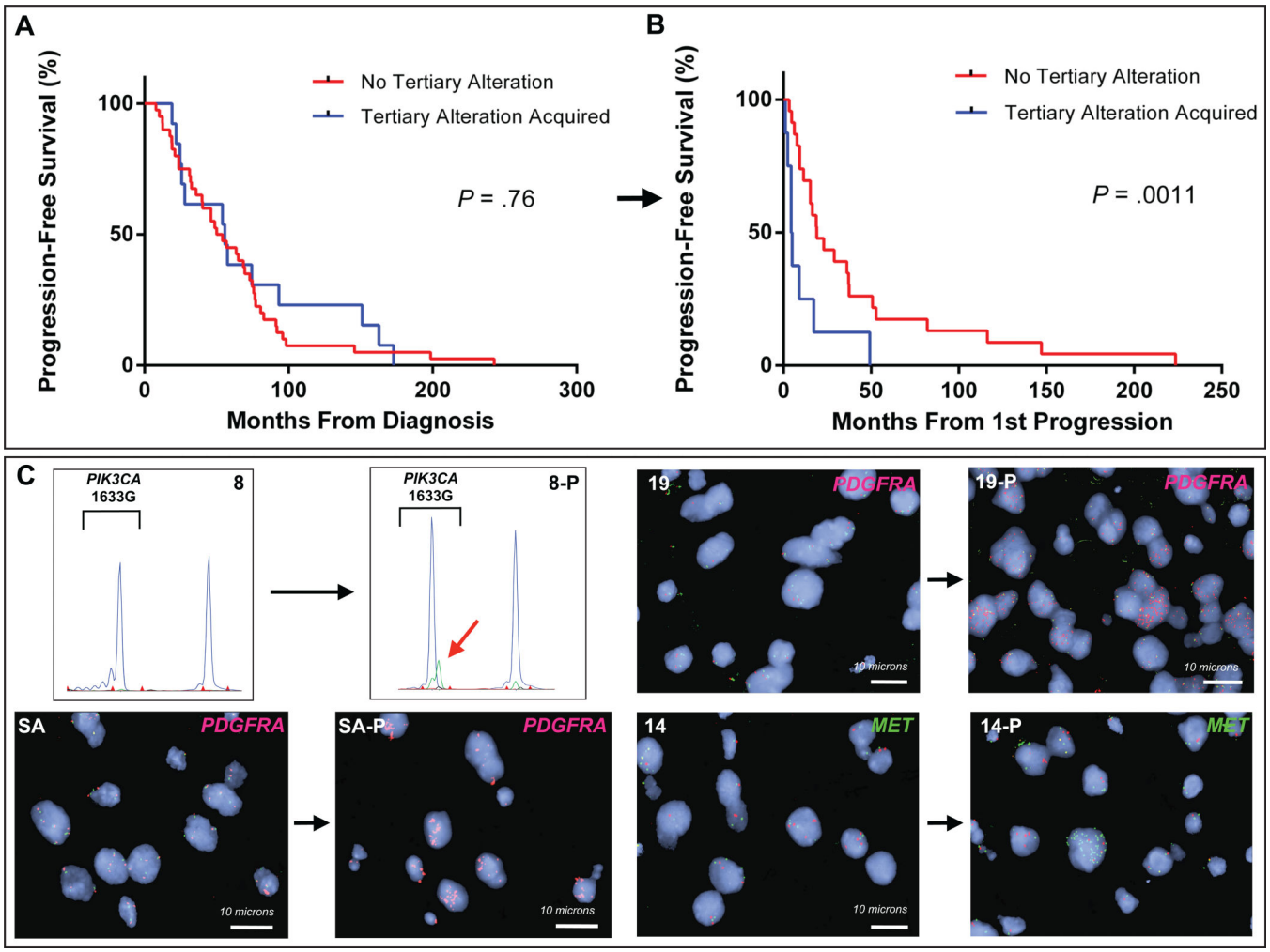

Figure 3. Tertiary alterations are acquired at progression and reduce subsequent progression-free survival

(A and B) Kaplan-Meier estimates of progression-free survival (PFS) in patients who had biopsy at initial diagnosis and at progression by presence of tertiary alteration. (A) PFS from the time of initial diagnosis and (B) from the time of progression. (C) SNaPshot and FISH images of matched patient tumors. Top left: SNaPshot images of patient 8 reveal wildtype *PIK3CA* E545 genotype in the initial tumor and *PIK3CA* E545K mutant allele (red arrow) in the progressive tumor (8-P). Bottom left: FISH images of patient SA initial and progressive (SA-P) tumor with *PDGFRA* probe (red) and CEN4 control probe (green). Top right: FISH images of patient 19 initial and progressive tumor (19-P) probed for *PDGFRA* (red) and CEN4 (green). Bottom right: Patient 14 initial and progressive (14-P) tumor probed with *MET* (green) and CEN7 control (red).

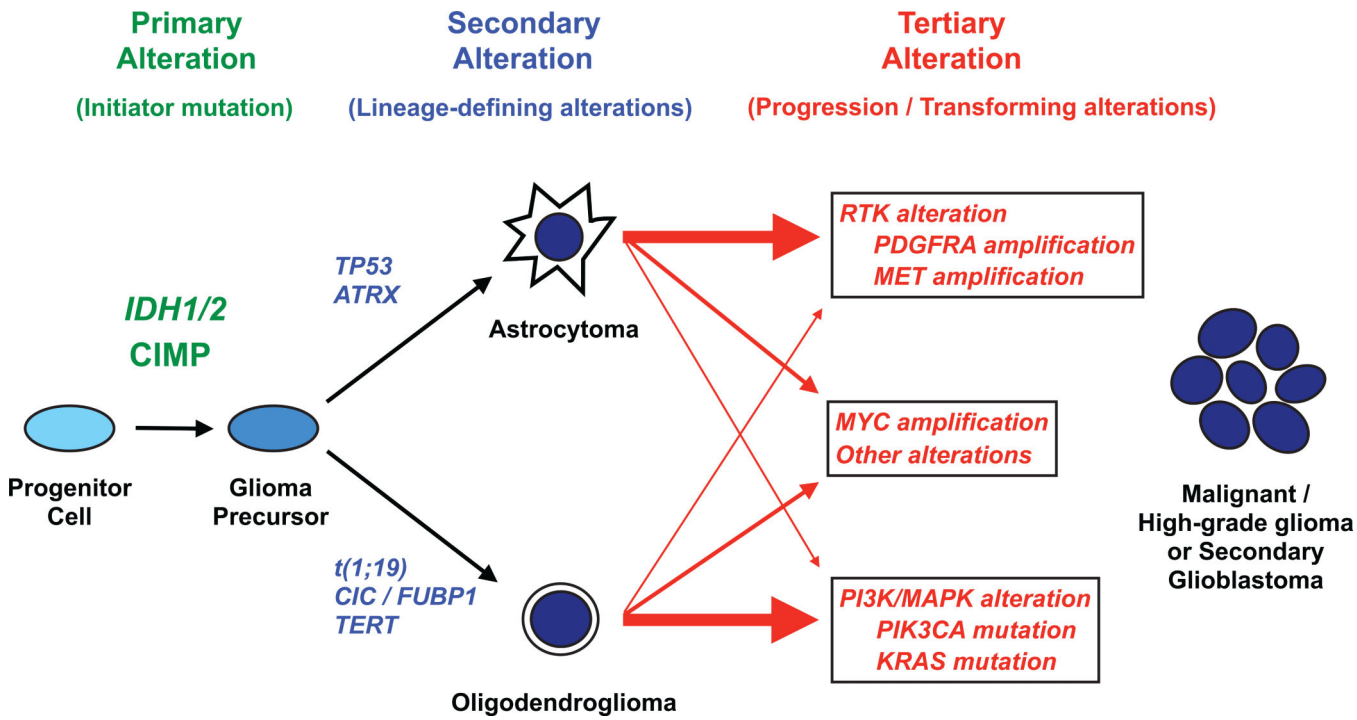

Figure 4. Molecular taxonomy of *IDH*-mutant glioma progression

We propose that *IDH*-mutant gliomas develop and progress through an ordered sequence of oncogenic alterations. *IDH*-mutant gliomas are initiated by the occurrence of *IDH1* or *IDH2* mutation and widespread hypermethylation of CpG islands (CpG island methylator phenotype, CIMP) in a glial progenitor cell population. The subsequent acquisition of *TP53* and *ATRX* mutations results in development along an astrocytoma pathway whereas the codeletion of 1p and 19q (t1;19) along with *CIC*, *FUBP1* and *TERT* mutations result in the formation of oligodendrogliomas. After acquisition of these “lineage-defining” mutations, *IDH*-mutant astrocytomas and oligodendrogliomas may follow several “tertiary” genetic pathways during the transformation to malignant or high-grade tumors. Astrocytomas tend to amplify growth receptor genes such as *PDGFRA* and *MET*, whereas oligodendrogliomas tend to develop activating mutations in intracellular signaling genes such as *PIK3CA* and *KRAS*. Alternative tertiary pathways include Myc activation and other undescribed mutations. Acquisition of tertiary genetic alterations may result in more malignant behavior. RTK, receptor tyrosine kinase; PI3K, Phosphoinositide 3-kinase; MAPK, mitogen-activated protein kinase.

Table 1

Orthotopically implanted patient IDH-mutant gliomas.

MGG	Histology	Sex	Age at Dx	Prior treatment	Time to xeno[a] (Mos.)	IDH1 mutation	Confirmed Secondary (Lineage) Alteration	MGMT	Tertiary Alteration
Generated Xenograft									
60	GBM-O	F	45	None	4	R132H	*CIC* mutant	M	*PIK3CA* H1047L
79	Recurrent AOA	M	33	RT, SRS	3	R132H (homozygous)	*TP53* mutant	n.t.	*PDGFRA* amp
88	Secondary GBM	F	41	RT, TMZ x 10 cycles, LBH589+BEV, CPT-11+BEV	6	R132H	*TP53* mutant	M	None detected
108	GBM-O	M	30	None	5	R132H	*TP53* mutant	M	*PIK3CA* R93Q
117	Secondary GBM	F	32	RT	3	R132H	*TP53* mutant	U	*PDGFRA* amp
119	Secondary GBM	M	56	RT	7	R132H	*TP53* mutant	M	None detected
132	Recurrent AOA	M	32	TMZ chemoradiation + 11 TMZ cycles	4	R132H	*TP53* mutant	U	*MET* focal amp
152	GBM with PNET component	M	34	Gliadel, TMZ chemoradiation	1	R132H	*TP53* mutant	M	*N-MYC* amp
No Xenograft									
71	AOA	M	51	None	−	R132H	1p/19q non-codel	M	None detected
78	LGO	M	41	None	−	R132H	1p/19q codel	M	None detected
81	GBM	M	27	None	−	R132H	*TP53* mutant	U	None detected
82	AOA	M	34	TMZ x 12 cycles	−	R132H	1p/19q codel	n.t.	None detected
83	Recurrent GBM	M	43	RT + gefitinib followed by gefitinib x 8 years	−	R132H	*TP53* mutant	n.t.	None detected
96	Recurrent AOA	M	24	TMZ chemoradiation + 6 TMZ cycles, isotretinoin x 10 cycles	−	R132H	*TP53* mutant	U	None detected
103	Recurrent AOA	M	26	PCV x 6 cycles then RT, TMZ x 7 cycles, BEV+TMZ x 12 cycles	−	R132H	1p/19q non-codel	M	None detected
109	Recurrent AO	F	35	TMZ x 12 cycles, RT	−	R132H	1p/19q codel	n.t.	None detected
116	AA	M	24	None	−	R132C	*TP53* mutant	U	None detected
124	LGOA	F	38	None	−	R132C	1p/19q non-codel	U	None detected
126	AO	F	56	None	−	R132H	1p/19q codel	n.t.	None detected
130	AOA	F	52	None	−	R132H	1p/19q codel	n.t.	None detected

Abbreviations: MGG, Mass General Glioma; Dx, diagnosis; Xeno, xenograft; Mos., months; GBM, glioblastoma; GBM-O, Glioblastoma with oligodendroglioma component; AOA, anaplastic oligoastrocytoma; AO, anaplastic oligodendroglioma; AA, anaplastic astrocytoma; LGO, low-grade oligodendroglioma, LGOA, low-grade oligoastrocytoma; PNET, primitive neuroectodermal tumor; RT,

radiation therapy; SRS, stereotactic radiosurgery; TMZ, temozolomide; BEV, bevacizumab; PCV, procarbazine, CCNU, Vincristine regimen; codel, codeleted; amp, amplified; M, methylated; U, unmethylated; n.t., not tested.

[a] months elapsed until 1st intracranial xenograft developed and became lethal.

Clin Cancer Res. Author manuscript; available in PMC 2014 December 01.

Table 2

Genetic alterations in IDH-mutant glioma patients at MGH.

Pt	Age at Dx	Sex	Initial Histology	Initial WHO Grade	OS (mos)	PFS (mos)	IDH1 mutation	Confirmed Secondary (Lineage) Alteration	Treatment Prior to Detection of Tertiary Alteration	Tertiary Alteration (amino acid substitution or copy number ratio[#])
1	60	M	Oligoastrocytoma	2	78.3*	21.9	R132H	codel	RT; TMZ (18 cycles)	*AKT1* (E17K), *KRAS* (G12R), *PIK3CA* (H1047L)
2	41	F	Astrocytoma	2	165.1*	54.0	R132H	codel	TMZ (12 cycles); RT	*KRAS* (G13D)
3	33	F	Oligodendroglioma	2	159.8*	159.8*	R132H	codel	PCV (6 cycles); RT	*KRAS* G12R)
4	54	M	GBM-O	4	38.4*	25.7	R132H	codel	None	*KRAS* (G12A)
5	43	M	Oligodendroglioma	2	180.4*	172.9	R132H	codel	None	*PIK3CA* (R88Q)
6	51	F	Oligodendroglioma	2	28.3*	24.6	R132H	codel	TMZ (12 cycles)	*PIK3CA* (E545G)
7	30	M	Anaplastic oligoastrocytoma	3	62.4*	55.7	R132H	NA	Concurrent RT/TMZ + adjuvant TMZ (12 cycles)	*PIK3CA* (E542K)
8	38	M	Anaplastic oligoastrocytoma	3	99.2*	74.4	R132H	codel	Concurrent RT/TMZ + adjuvant TMZ (12 cycles); TMZ (10 cycles)	*PIK3CA* (E545K)
9	39	F	Anaplastic oligodendroglioma	3	166.0*	162.7	R132H	no codel	PCV (6 cycles); RT	*PIK3CA* (R88Q)
10	45	F	GBM	4	8.1*	8.1*	R132H	codel	None	*PIK3CA* (H1047Q)
11	51	M	GBM	4	0.7*	0.7*	R132H	NA	None	*PIK3CA* (H1047R)
12	29	M	GBM-O	4	12.2*	12.2*	R132H	no codel	None	*PIK3CA* (R93Q)
13	34	M	Anaplastic oligoastrocytoma	3	31.3	28.0	R132H	*TP53* V272M	Concurrent RT/TMZ + adjuvant TMZ (12 cycles)	*MET* amplification (5:1 in 10-15% cells)
14	52	F	GBM	4	113.2*	93.2	R132H	NA	Concurrent RT/TMZ + adjuvant ddTMZ (25 cycles)	*MET* amplification (>25:1 in 1/50 cells)
15	33	M	GBM with PNET component	4	5.0	3.9	R132H	*TP53* R273H	None	*N-MYC* amplification (>25:1)

Pt	Age at Dx	Sex	Initial Histology	Initial WHO Grade	OS (mos)	PFS (mos)	IDH1 mutation	Confirmed Secondary (Lineage) Alteration	Treatment Prior to Detection of Tertiary Alteration	Tertiary Alteration (amino acid substitution or copy number ratio[#])
16	35	M	Anaplastic astrocytoma	3	24.4[*]	24.4[*]	R132H	*TP53* R273C	None	*PDGFRA* amplification (>25:1 in 1/200 cells)
17	47	M	Anaplastic astrocytoma	3	58.5[*]	57.5	R132H	no codel	Concurrent RT/TMZ + adjuvant TMZ (6 cycles)	*PDGFRA* amplification (>25:1)
18	45	M	GBM	4	25.6[*]	25.6[*]	R132H	*TP53* R273C	None	*PDGFRA* amplification (>25:1)
19	32	F	Astrocytoma	2	79.6	19.1	R132H	*TP53* R273C	RT	*PDGFRA* amplification (>25:1)
20	61	M	GBM-O	4	9.4[*]	9.4[*]	R132H	*TP53* R273C	None	*PTEN* (R173C)

Abbreviations: MGH, Massachusetts General Hospital; Pt, patient; Dx, diagnosis; OS, Overall Survival; PFS, Progression-free survival; mos, months; GBM, glioblastoma; GBM-O, glioblastoma with oligodendroglioma component; PNET, primitive neuroectodermal tumor; codel, 1p/19q codeleted; TMZ, temozolomide; ddTMZ, dose dense temozolomide; RT, radiation therapy; NA, not available

[*] Event has not yet occurred;

[#] ratio of specific gene probe to centromere control.